

Non-buoyant microplastic settling velocity varies with biofilm growth and ambient water salinity

Freija Mendrik ^{1✉}, Roberto Fernández², Christopher R. Hackney ³, Catherine Waller¹ & Daniel R. Parsons⁴

Rivers are the major conveyor of plastics to the marine environment, but the mechanisms that impact microplastic (<5 mm) aquatic transport, and thus govern fate are largely unknown. This prevents progress in understanding microplastic dynamics and identifying zones of high accumulation, along with taking representative environmental samples and developing effective mitigation measures. Using a suite of settling experiments we show that non-buoyant microplastic settling is influenced by a combination of biofilm growth, water salinity and suspended clay concentrations typically seen across fluvial to marine environments. Results indicate that biofilms significantly increased settling velocity of three different polymer types of non-buoyant microplastics (fragments and fibres, size range 0.02–4.94 mm) by up to 130% and significant increases in settling velocity were observable within hours. Impacts were both polymer and shape specific and settling regimes differed according to both salinity and sediment concentrations. Our results further validate previous statements that existing transport formula are inadequate to capture microplastic settling and highlight the importance of considering the combination of these processes within the next generation of predictive frameworks. This will allow more robust predictions of transport, fate and impact of microplastic pollution within aquatic environments.

¹Energy and Environment Institute, University of Hull, Hull, UK. ²Department of Civil and Environmental Engineering, The Pennsylvania State University, State College, PA, USA. ³School of Geography, Politics and Sociology, Newcastle University, Newcastle, UK. ⁴Loughborough University, Loughborough, UK.
✉email: F.Mendrik@hull.ac.uk

Estimates of plastic flux entering the ocean annually vary between 4.8 to 12.7 million metric tons, while floating marine plastic is calculated to be only 268,940 tons, accounting for just 2–6% of the estimated plastic entering aquatic systems every year^{1,2}. Land-based sources such as mismanaged waste, have resulted in rivers becoming a major pathway for macro- (>5 mm) and micro- (<5 mm) plastic pollution to enter the marine environment^{1,3}. Yet, as microplastics, move through a river basin and transfer to the marine environment, they will undergo a range of environmental gradients and physical, biological and chemical transitions, including changes in salinity and sediment concentrations. Additionally, weathering, such as fragmentation through physical stress and UV exposure, and biofilm growth will also impact the dynamics of microplastics through the water column and wider aquatic system^{4–6}.

The likelihood that a given microplastic particle will settle out of suspension when entering an aquatic environment varies depending on the physicochemical, hydrodynamic and biological conditions of the environment^{7,8}. First, microplastic distribution is dependent on a suite of polymer properties (such as density, shape, size), but as subsequent growth of surficial biofilm occurs within minutes to hours of entering an aquatic system^{9,10} (Fig. 1), the density of the microplastic particle can change rapidly through time. This results in alterations to particle buoyancy and thus relative density to the ambient fluid, which has considerable implications in varying a particle's trajectory in the water column^{11–15}. Furthermore, the development of flocs, and further associated changes in density and particle size, is known to affect the settling velocity of particles, particularly in river to estuary transition zones¹⁶. While silts and clays that undergo flocculation are typically 0.06 mm or smaller in size, flocculation can occur at larger grain sizes, including sand^{17,18}. With surficial biofilms, microplastic particles can also become part of hetero-aggregates (or flocs), which includes other naturally suspended sediment^{19,20}. Indeed, Besseling et al.²¹ has demonstrated the

aggregation of 70 and 1050 nm polystyrene particles with clay in natural freshwaters. However, the impact of floc formation on microplastic distribution, settling and fate is currently unquantified for larger particles and within saline waters^{19,22,23}.

Changes in salinity and suspended sediment that occur across a freshwater-marine boundary is known to affect the development of flocs and thus overall settling velocity of particles, especially as the relative density of the particle changes as it moves into denser saline water^{24–27}. As water becomes more saline (and water density increases), particles are more likely to stay suspended within the water column, although this also depends on physical influences such as flow velocity and turbidity. Settling velocity is thus a key parameter used to predict sediment transport pathways, yet no comprehensive study has yet experimentally quantified the combination of these effects (biofilm, salinity and sediment concentration) for microplastics (Supplementary Table 1)^{4,22,28–33}.

Here, we experimentally quantify how microplastic settling velocities vary through time as a function of biofilm growth and as they transition from freshwater to saline conditions in addition to experiencing various sediment concentrations typically found in estuarine environments. The change in conditions was tested here as the majority of microplastics originate from land-based sources, and therefore will undergo a range of environmental conditions. The various salinity and suspended sediment conditions were tested to ensure the experiments were environmentally relevant as possible, as the majority of microplastics originate from land-based sources and will therefore undergo these environmental changes as they transition from fluvial to marine systems. Three non-buoyant microplastics types were tested: polyethylene terephthalate (PET), polyvinyl chloride (PVC) fragments and nylon, polyester and acrylic (NP&A) fibres. It is acknowledged that there are several other common polymers frequently found in aquatic environments. However, preliminary experiments that included buoyant microplastics (polystyrene

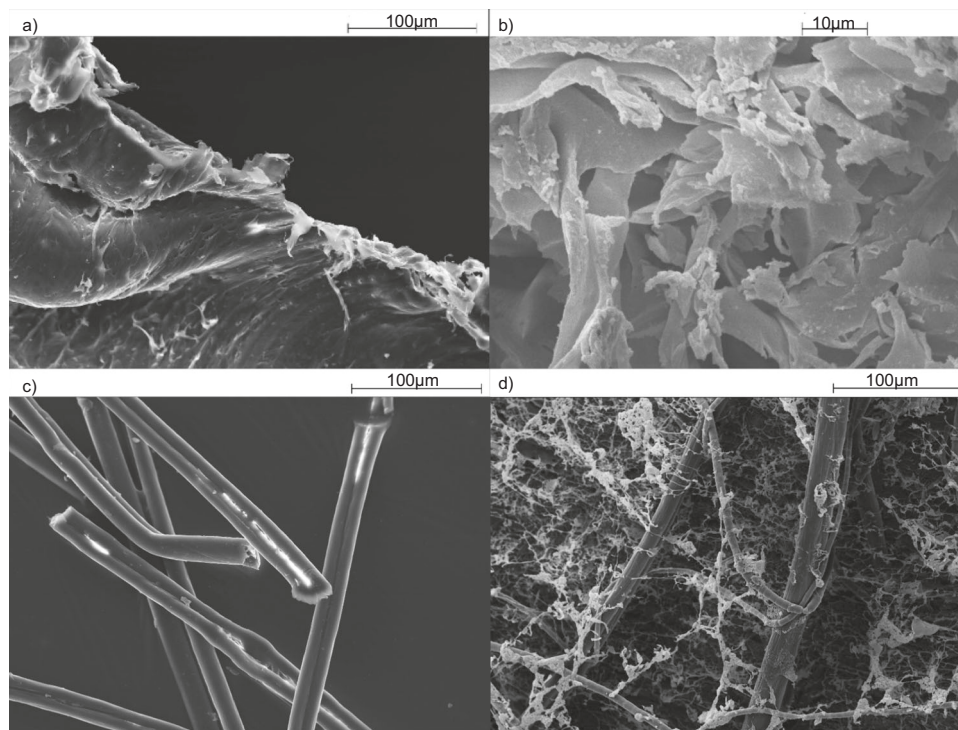


Fig. 1 SEM images of microplastics before and after biofilm colonisation. **a** Clean polyethylene terephthalate (PET), **b** biofilmed PET, **c** clean nylon, polyester and acrylic (NP&A) fibres and **d** biofilmed NP&A fibres. Note the scale in **b** is different than in **a**, **c**, **d** due to the higher magnification needed to visualise the biofilmed PET.

(PS), polypropylene (PP) and high-density polyethylene (HDPE)) showed that the majority of these particles remained buoyant even after biofouling. Therefore this study focused on the subset of non-buoyant particles which are regularly found in aquatic environments. However, it should be noted that buoyant polymers may become non-buoyant after additional environmental processes such as photodegradation that may alter buoyancy over time and should be considered in future studies. Using high-resolution measurements of particle settling velocities, we demonstrate how biofilm growth, changes in salinity and sediment concentration impact microplastic settling velocities, and show how these impacts are polymer and shape specific. Furthermore, our analysis reveals that widely applied sediment transport formulae^{34–37} are inaccurate for predicting microplastic fate and transport; microplastic interactions with—and relative density changes due to—biofouling, as well as salinity and sediment concentration changes, are not well constrained for microplastics in sediment transport laws.

Results and discussion

Biofilm and particle shape impacts. To evaluate the controlling factors that influence microplastic transport, a series of settling experiments measuring particle settling velocity (see full Methods for details) were conducted; testing fragment and fibre polymer types and shapes, the impact of biofouling, salinity, and suspended sediment concentrations on settling velocity. Comparisons were made between clean and biofilmed particles under varying salinity and clay concentrations to understand the effects of biofouling under different conditions. The impacts of salinity and clay concentrations were also evaluated for clean and biofilmed particles separately. Comparisons were considered significant when $p < 0.05$ and are summarised in Supplementary Table 2. Biofilm time trials were also conducted to understand how quickly the impacts of biofilms on settling velocities are realised.

The settling of microplastics was shape dependant as clean fibres settled considerably slower than fragments (Fig. 2) despite the density range of the fibres being fairly similar to the fragments (NP&A = $1.01\text{--}2.30\text{ g cm}^{-3}$, PET = 1.39 g cm^{-3} and PVC = 1.44 g cm^{-3}). The impacts of particle shape on settling has been shown previously, where Khatmullina et al.³¹ highlighted that the different shapes of particles highly influences sinking behaviours of microplastics and the need for further investigation of environmentally relevant particles, yet did not test textile fibres. Few microplastic settling experiments include fibres, but recently, Van Melkebeke et al.³⁸ demonstrated that sinking velocities of fibrous microplastics are significantly inhibited due to their shape and higher drag coefficient, which is supported by this study³⁸.

However, biofilm growth had the greatest impact on microplastic settling across all salinities and clay concentrations and increased the settling velocity on average by 40%. Furthermore, the magnitude of this change was different between polymer types (see Supplementary Table 2 for statistical summary). Settling velocity increased significantly between clean and biofilmed PET fragments at all salinities (ppm, SAL): at SAL0 settling increased by 73%, at SAL18 by 29% and at SAL30 by 55%. A significant increase in settling velocity due to biofouling was also observed at all clay concentrations: 83% at 0 mg, 27% at 100 mg, 67% at 400 mg and 64% at 600 mg clay (Fig. 2a). However, for PVC fragments, the significant increase in velocity between clean and biofilmed particles was seen for fewer scenarios: 25% at SAL30, 13.5% at 0 mg and 68% at 600 mg clay (Fig. 2b). There was also a reduced effect of biofouling on nylon, polyester and acrylic (NP&A) fibres with a significant increase in settling velocity observed for only two scenarios: 55% at SAL30 and 132% at 400 mg clay (Fig. 2c).

Biofilm growth causes microplastics to settle faster due to an increase in particle specific density, not area (Supplementary Figs. 1–3), which has been observed before^{4,14,30,39,40}. Biofouling was hypothesised to cause microplastics to become more cohesive and form flocs with siliclastic grains, leading to an observable increase in particle size⁴¹, yet this was not seen. Lagarde et al.¹² highlighted that studies have previously shown that the growth of biofilms and consequent hetero-aggregate formation is highly dependent on microplastic polymer chemical nature (polymer type). Polypropylene (PP) fragments were more likely to form heteroaggregates with freshwater algae compared to high-density polyethylene (HDPE), potentially due to different types of biofilm (EPS) being produced¹². The chemical composition and surface texture of PET is also likely to have provided a preferred medium for microbes to grow on compared to PVC and NP&A fibres. This is reflected in the results, where compared to PET fragments, PVC fragments and NP&A fibres were less impacted by biofilm colonisation (Fig. 2)⁴. This highlights the need for future studies to investigate a range of particle types as impacts on microplastic settling are highly dependent on the polymer composition.

The impacts of biofilms on microplastic settling velocity occur quickly and can be seen in less than a week, as demonstrated by our time trials (see ‘Methods’): PET fragments were biofouled and settling velocity measured over 0–8 weeks (Fig. 3). Settling velocity increased considerably by week 1 with average settling velocity of PET fragments being $16.85 \pm 0.92\text{ mm s}^{-1}$ (\pm values represent standard error) at week 0 (clean), increasing to $29.38 \pm 1.16\text{ mm s}^{-1}$ at week 1 and $36.67 \pm 1.95\text{ mm s}^{-1}$ at week 2. In fact, biofilm growth caused a significant difference between week 0 and 1 ($p < 0.001$), week 0 and 2 ($p < 0.001$), week 0 and 4 ($p < 0.001$), week 0 and 8 ($p < 0.001$) and between week 1 and 2 ($p = 0.04$). This demonstrates how the dynamics of microplastics settling rates are fundamentally controlled by time. Impacts of biofouling can occur quickly, within a week and remain similar from week 2 onwards, highlighting the need for experiments and modelling to consider how microplastic settling changes with environmental exposure

Microplastic settling behaviour changes across the freshwater–marine salinity gradient. Our results reveal that non-buoyant microplastic settling velocity is influenced by changes in salinity and sediment concentration (Fig. 2) that could be experienced as microplastic particles cross the freshwater–marine boundary. It is clear that multiple environmental and biological conditions need to be considered when predicting microplastic transport. For clean PET fragments, settling velocity was significantly higher at SAL18 ($15.8\text{ mm s}^{-1} \pm 0.54$), compared to SAL0 ($13.1\text{ mm s}^{-1} \pm 0.40$) and SAL30 ($12.7\text{ mm s}^{-1} \pm 0.49$). This highlights how salinity impacts microplastic settling, but requires further investigation. However, for biofouled particles, settling velocity was considerably higher at SAL0 ($22.74\text{ mm s}^{-1} \pm 0.76$) compared to SAL30 ($19.68\text{ mm s}^{-1} \pm 0.67$). The influence of salinity was much more varied for PVC fragments, with clean particles settling rates significantly lower at SAL30 ($17.67\text{ mm s}^{-1} \pm 0.78$) compared to SAL0 ($24.90\text{ mm s}^{-1} \pm 1.10$) as expected. Biofilmed PVC fragments settled significantly faster at SAL0 ($25.67\text{ mm s}^{-1} \pm 0.98$) compared to SAL18 ($23.05\text{ mm s}^{-1} \pm 0.97$) but salinity had less of an impact on biofilmed PVC fragment settling compared to biofilmed PET particles. Finally, no significant effect on settling rate due to salinity was observed for NP&A fibres. Polymer-specific salinity impacts have been shown previously, with higher salinity leading to lower settling velocities for certain polymers³⁰. Salinity lowers settling velocity for polystyrene (PS) particles, yet for higher density polymers such as PET and PVC salinity had less of an impact³². Conversely, Wang et al.⁴² described how an increase in salinity only had

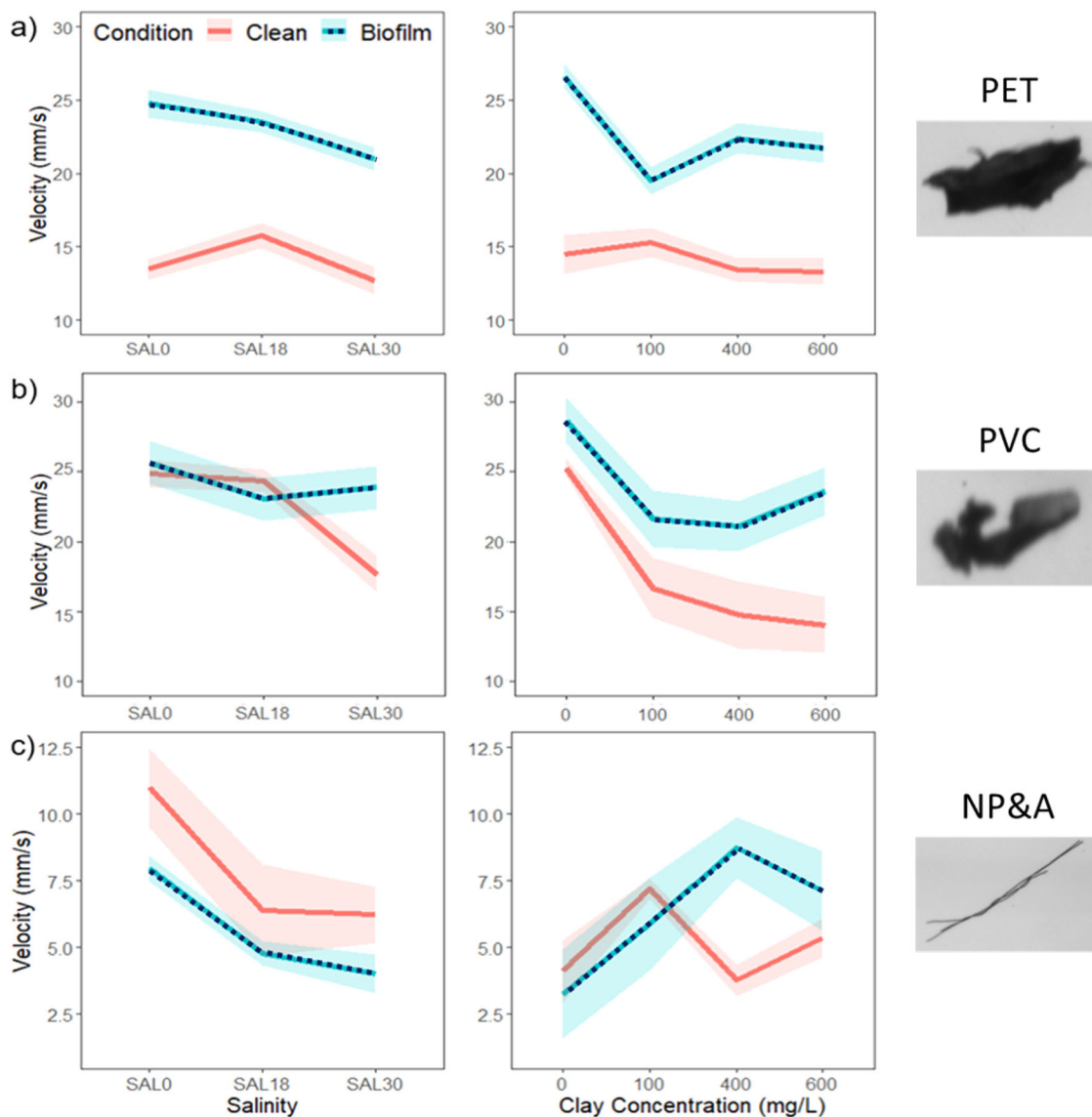


Fig. 2 Main effects plot of condition, salinity and clay concentration on non-buoyant microplastics. **a** Polyethylene terephthalate (PET), **b** polyvinyl chloride (PVC), and **c** nylon, polyester and acrylic (NP&A) fibre microplastics. Solid lines indicate mean plots, while the shaded areas indicate confidence bands for all points. Red solid lines and shading are for clean particles, while blue dashed lines and shading are for biofilmed particles. For PET $n = 1796$, PVC $n = 1015$ and NP&A $n = 1111$. Note that for **c** the scale range is smaller as settling velocity was considerably lower for NP&A fibres.

minor impacts on PET but showed impacts on PVC, lowering the settling velocity. This is similar to our results, especially clean PET and PVC particles, with salinity having much more impact on clean PVC fragments compared to PET. However, our results show the much greater impact of biofilm growth on these relationships. As NP&A fibres have a lower density, a decrease in settling due to increase in salinity was expected, yet this was not seen perhaps due to the shape and surface area of fibres compared to spheres and fragments⁴. The results presented indicate that the settling regimes for non-buoyant microplastics differ as they undergo changes in environmental conditions that may occur across freshwater to marine environments. Therefore, the varying settling regimes must be considered when sampling and predicting the transport and fate of microplastics within these environments, in addition to changes in ecological risk.

Within the suspended sediment experiments, aggregation of microplastics and kaolinite was not observed as particle size did not increase (see Supplementary Figs. 1–3). However, settling velocity was still impacted. For PET and PVC fragments, overall

settling decreased with higher sediment concentrations but for NP&A fibres the impacts were more variable (Fig. 2). Again, patterns differed between polymers and whether microplastics were biofouled or not. Settling velocity remained similar for clean PET particles across all sediment concentrations and significant changes in settling velocity only occurred for biofilmed PET fragments. Highest settling rates occurred at 0 mg ($26.60 \text{ mm s}^{-1} \pm 1.21$) and statistical significance was observed between 0 mg and 100 mg ($19.50 \text{ mm s}^{-1} \pm 0.93$) and 0 mg and 600 mg ($21.73 \text{ mm s}^{-1} \pm 1.25$). For clean PVC, settling rates were considerably higher at 0 mg ($25.28 \text{ mm s}^{-1} \pm 0.77$), compared to 400 mg ($14.73 \text{ mm s}^{-1} \pm 0.81$) and 600 mg ($14.04 \text{ mm s}^{-1} \pm 1.00$). For PVC, the highest settling rate was also observed at 0 mg for biofilmed PVC fragments ($28.69 \text{ mm s}^{-1} \pm 1.13$) compared to 100 mg ($21.66 \text{ mm s}^{-1} \pm 1.06$), 400 mg ($21.12 \text{ mm s}^{-1} \pm 1.25$) and 600 mg ($23.60 \text{ mm s}^{-1} \pm 1.09$). The decrease in settling velocity of PET and PVC fragments with clay mixing was not predicted. The surface properties of fragmented microplastics, such as charge and a rough surface may cause friction and will therefore play an

important role in how they are transported and must be considered when predicting microplastic transport⁴³. The mixing of kaolinite and microplastics may have caused abrasion

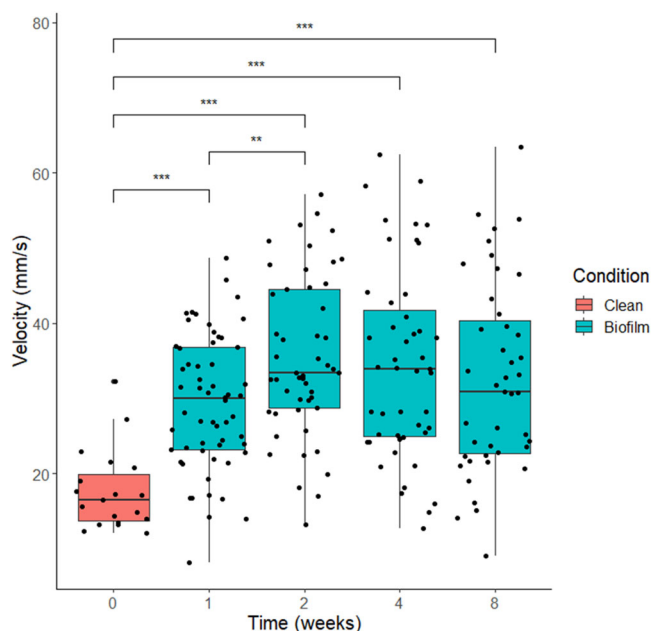


Fig. 3 Changes in settling velocity of polyethylene terephthalate (PET) fragments over time (0–8 weeks) due to biofilm growth. Clean particles are indicated by the red box while biofilmed particles are represented by the blue boxplots. The boxes represent the interquartile range where the line within each box represents the median and the whiskers represent the minimum and maximum. Brackets demonstrate statistical significance: *** $p < 0.001$ and ** $p < 0.05$ ($n = 216$).

(Supplementary Fig. 4) and further deviation from a spherical shape, which creates a larger surface area that induces greater friction drag that is likely to lower particle settling velocity^{32,44}. Also, the drag coefficient may have increased due to a small amount of clay attaching to the particles. Flocs may have also formed in the mixing procedure but as the rate of aggregation strength of flocs depends on electrical charge of particles, perhaps the forces between particles here were weak and caused flocs to break down during transfer or deposition in the settling column²⁴, or the electrochemical forces between clay and polymer particles are not as strong and need to be studied further. The attachment efficiencies and subsequent formation of microplastic and sediment heteroaggregates has been demonstrated by Besseling et al.²¹. However, the microplastics tested were 70 and 1050 nm PS, much smaller than those in this study and highlights the need for a broader range of sizes to be tested in the future.

For NP&A fibres, the impact of clay concentration was very different compared to the other polymers. The highest settling occurred at 100 mg for clean NP&A fibres, ($7.20 \text{ mm s}^{-1} \pm 0.48$) but was only significantly different to 400 mg ($3.76 \text{ mm s}^{-1} \pm 0.22$). However, for biofilmed NP&A fibres, settling rate was highest at 400 mg ($8.44 \text{ mm s}^{-1} \pm 1.01$) and lowest at 0 mg ($3.25 \text{ mm s}^{-1} \pm 0.46$) with significant differences between 0 mg and 100 mg ($5.90 \text{ mm s}^{-1} \pm 0.51$), 400 mg ($8.73 \text{ mm s}^{-1} \pm 1.02$) and 600 mg ($7.12 \text{ mm s}^{-1} \pm 0.70$). Kaolinite particles have been observed to adsorb onto the surface of polystyrene latex microspheres 1 μm in diameter which may have occurred here, increasing density and settling, yet overall particle size/area was not altered significantly⁴⁵. It should be noted that some fibres did clump (Supplementary Fig. 5) and this made calculation of settling difficult, which may have impacted the results. Fibres may clump and tangle in turbulent conditions, so this should be considered for future studies. No PET or PVC particles were observed to clump together in this way.

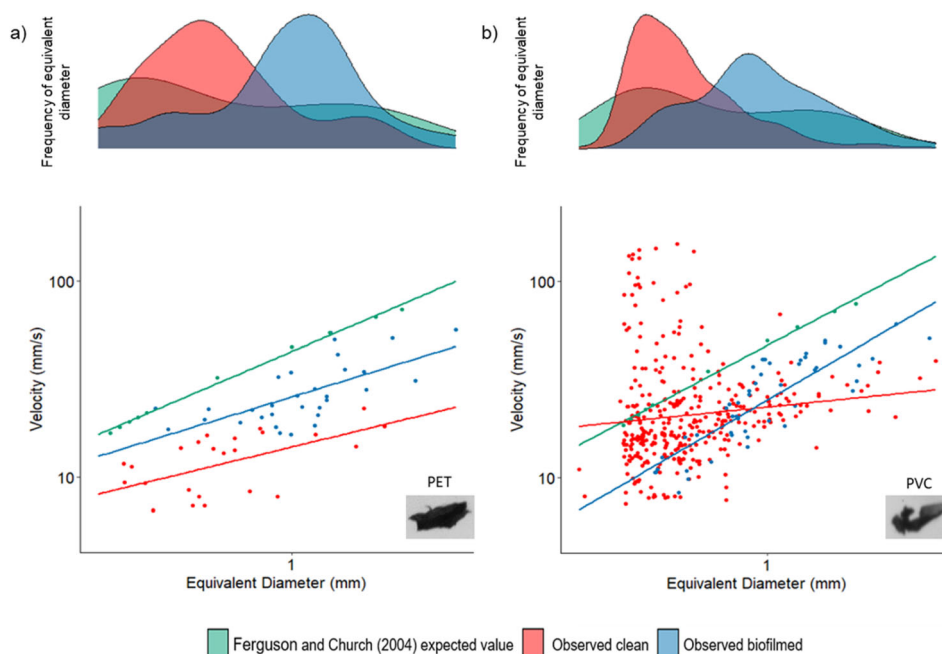


Fig. 4 Expected settling velocity calculated using Ferguson and Church compared to our observed experimental values for clean and biofilmed microplastics. **a** Polyethylene terephthalate (PET) ($n = 38$) and **b** polyvinyl chloride (PVC) ($n = 383$). The expected settling velocity of particles calculated using Ferguson and Church³⁷ is indicated by the green solid lines, points and shading, the observed experimental clean particle values are shown by solid red lines, points and shading and the observed experimental biofilmed particle values are indicated by the solid blue lines, points and shading. Marginal density plots indicate the distribution of velocity and equivalent diameter data. This highlights that grain size variation must be included in predictive models.

Comparison with empirical predictions. It has been argued that microplastics in aquatic systems will behave in a way that is comparable to natural sediment and therefore microplastic fate can be predicted using the same methods available for natural particles^{4,46,47}. To assess this, we compare our results to a widely applied universal sediment transport formula that resolves Stokes' Law for fine grained sediment transport and turbulent fluid motion for larger grains to determine grain settling velocity (see 'Methods')³⁷. The theoretical settling velocity was calculated to be much higher compared to both clean and biofilmed experimental results for all sizes of PET (Fig. 4a). This supports previous studies such as Waldschlager and Schüttrumpf³³ and Van Melkebeke et al.³⁸ who also observed overestimation of theoretical values. Any models using this formula⁴⁸ will over-predict settling of PET microplastics resulting in a greater microplastic load in suspension than would be expected. For PVC microplastics, the formula both over and under-predicted settling velocities depending on particle size (Fig. 4b). Sediment equations could be used if the microplastics have hydraulically equivalent physical properties⁴⁹, however microplastics exist in a much wider range of shapes than natural sediment grains. The expected values were different for observed particles settling, especially fibres, probably due to a lack of shape descriptors. Van Melkebeke et al.³⁸ demonstrated the need for sufficient shape descriptors, especially sphericity and circularity, to accurately predict microplastic settling for a range of polymer shapes. Despite Waldschlager and Schüttrumpf's³³ development of a new formula for settling of microplastics, we were unable to make comparisons using their predictions as they rely on needing 3-axis dimensions for individual particles and do not consider the impacts of biofouling, which we have shown as a first order control. Van Melkebeke et al.³⁸ also showed that although Waldschlager and Schüttrumpf's³³ formula had sufficient shape descriptors for several polymer shapes, it was not accurate for films. Indeed, our physical experiments highlight the need for a new generation of transport formulae that consider irregular microplastic shapes, biofouling and the high sensitivity to changes in salinity. Currently, although advances have been made, the complex mechanisms that control microplastic transport and fate are poorly understood, which hinders our ability to manage and protect aquatic environments. Models do exist to quantify microplastic settling specifically (such as the Kooi model that simulated the effects of biofouling on sinking⁵⁰), yet they do not include predictions across salinity gradients or consider impacts of suspended sediment that occur in aquatic environments. Here we demonstrated that biofouling is a first order control on the settling velocity of microplastics (with impacts observed over only a few days) across a range of salinities and clay concentrations that replicate riverine and marine conditions. The effect varies by polymer type and ambient conditions (salinity/clay concentration), and evolves in time. This further highlights that the changes in microplastic settling regimes from a riverine to marine environment must be appreciated to precisely predict microplastic fate and the formation of any high concentrations zones in the environment.

Although herein we only explore three types of non-buoyant microplastic, the results demonstrate a suite of unique and important insights into non-buoyant aquatic microplastic transport under experimental conditions. Future work should build on the methods explored here, testing a wider range of microplastic polymers, perhaps those from environmental samples, in addition to buoyant polymers in order to gain a more comprehensive understanding of microplastic settling in aquatic environments. A range of size fractions must also be further tested, especially for their ability to aggregate with suspended siliciclastic sediments²¹. Other types of sediment, such as sand, types of clays and

carbonates, should also be investigated for their impact on microplastic transport.

While available sediment transport formulae are useful for basic plastic transport predictions, we support and unequivocally show they are largely inaccurate and must be urgently updated to incorporate these key factors identified herein into new predictive frameworks, particularly biofouling, salinity impacts and time functions. This would allow more robust predictions of microplastic fallout and retention in fluvial systems and therefore more precisely forecast microplastic loads into estuaries, coastal seas and oceans along with improving projections of microplastic fate^{1,3}. In turn, this would improve monitoring and sampling campaigns and enhance, future assessments of ecological impact of plastics through the freshwater-marine transition.

Methods

The microplastic particles. The majority of observed plastics in riverine systems are from packaging of a range of polymer densities, as turbulence of rivers allows polymers to remain buoyant⁵¹. Therefore, polymer types commonly found across freshwater and ocean environments, including beaches, sediment and epipelagic areas were chosen for the settling experiments⁵¹. Three types of plastic polymers were selected: fragments of polyethylene terephthalate (PET) (1.39 g cm^{-3}), and polyvinyl chloride (PVC) (1.44 g cm^{-3}), (Direct Plastics Limited, Sheffield, UK) were generated using a carving file. This ensured fragmentation of plastic and heterogeneous shapes and sizes that replicates environmental degradation of microplastics¹¹. PET is often used in packaging and PVC is widely used within construction, transport, healthcare and packaging and are both regularly found in aquatic systems. Fibres were generated from nylon, polyester and acrylic (NP&A) yarn ($1.01\text{--}2.30 \text{ g cm}^{-3}$) (The Knitting Network, Sittingbourne, UK). Fibres are one of the most commonly found microplastic type in aquatic systems, often due to washing of clothes releasing fibres and contaminating wastewater⁵². The properties of the polymers used in the experiments are summarised in table 1. Fragments and fibres were generated to be in the typical size range of microplastics commonly found in aquatic environments. In addition, irregular shapes of microplastics were chosen instead of pellets and spheres, to represent weathered and degraded plastics more typically found in aquatic environment. This allowed an estimate of settling velocities of microplastic particles that resemble those found in aquatic environments.

To colonise biofilms on microplastic particles, the methods of Hoellin et al.⁴ were adapted. Benthic sediment and overlying water was collected from the Humber River, Hull, UK. Fifty grams of benthic sediment and 200 ml of river water was placed in flasks with microplastics in a shaking incubator for 10 days at 37°C , 200 rpm. The flasks were then left at room temperature for 6 months. It should be noted that fibres are known to have significantly less bacterial abundance in biofilm colonisation compared to fragments and pellets⁴ and it was therefore expected that there would be less biofilm formation on fibre samples. Examples of plastics before and after biofilm growth are shown in Fig. 1.

To initiate the formation of flocs, kaolinite, a type of clay particle typical and abundant in environments was chosen and mixed with high concentrations of clean and biofilmed microplastics, with each polymer kept separate, in 200 ml conical flasks. The sediment range of $100\text{--}600 \text{ mg l}^{-1}$ was chosen from data collected by the Mekong River Commission⁵³ and incorporates suspended sediment concentrations found from fluvial to delta environments of one of the top contributing rivers to marine plastic pollution. To replicate turbulent flow, the sediment-microplastic mixtures were shaken horizontally at 300 rpm for 5 min then 150 rpm for 20 min. To ensure the any flocs formed held together, particles were extracted from the beakers with a glass pipette while they were still being shaken at 80 rpm and dropped in the water column (see below).

Experimental set-up. The settling velocity of the microplastic particles was determined through a series of non-intrusive sinking experiments conducted in a Laboratory Spectral Flocculation Characteristics (LabSFLOC) plexiglass column with dimensions of $12 \text{ cm} \times 12 \text{ cm} \times 33 \text{ cm}$ (Fig. 5, analogous to previous settling velocity experiments^{22,29–31,33,38,54–56}). The LabSFLOC settling column is

Table 1 Summary of microplastic properties used to settling experiments.

Polymer	Density (g cm^{-3})	Size range (mm)
Polyethylene terephthalate (PET)	1.39	0.02–4.20
Polyvinyl chloride (PVC)	1.44	0.04–4.94
Nylon, polyester and acrylic (NP&A)	1.01–2.30	0.02–0.59

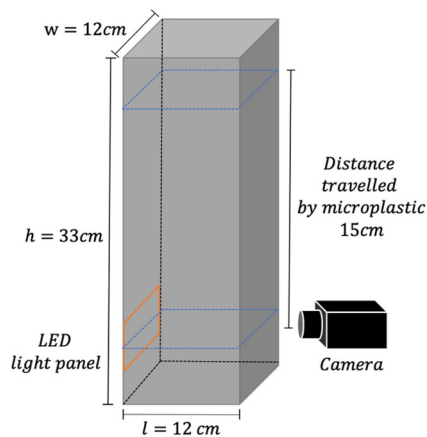


Fig. 5 Schematic of the Laboratory Spectral Flocculation Characteristics (LabSFLOC) experimental set-up. The set-up includes a plexiglass column of height 33 cm with a square cross section of 12 × 12 cm, filled with deionised water of varying salinities.

combined with a LED light panel (9 × 7 cm) and high-resolution video camera with a field of view of approximately 13 mm (Fig. 5) that collects particle settling video data that is processed to understand size, shape and velocity of individual particles and flocs (detailed below). This is the first time a LabSFLOC water column has been used for microplastic settling experiments and allows individual particles to be easily analysed for their settling behaviour and aggregation. It is comparable to previous microplastic settling experiments that have utilised similar water columns.

The LabSFLOC water column was filled with distilled water and the addition of sodium chloride (NaCl) to create salinities ranging from SAL0-30 to represent the change in salinity from a freshwater to marine environment. Distilled water was utilised to ensure no impurities were impacting microplastic transport. The water was left to settle for at least 15 min before each experimental run to ensure consistency. Before each experiment, microplastics were immersed in water of the same salinity and temperature used in the experimental water column in glass petri dishes to ensure no electrostatic discharge from particles, which may prevent or alter sinking behaviour³⁰. For the experiment, clean and biofilmed microplastics were placed with tweezers 0.01 m below the water surface of the LabSFLOC column to prevent any restraint caused by surface tension and left to move freely. For microplastics that were being tested under different sediment concentrations, a glass pipette was utilised for transferring particles so not to disturb any formed flocs. A series of images were taken of the particle movement. A minimum of 13 particles per condition were recorded for PET and PVC experimental series, with the majority having at least 100 counts. The measurement of a single particle movement was not repeated. For fibres, particles tended to clump together which made analysis of movement difficult. Therefore at least 5 particles were recorded per variable for fibre analysis. For PET total $n = 1796$, PVC $n = 1015$ and NP&A $n = 1111$. Particles travelled at least 15 cm before image recording took place to ensure microplastics had reached terminal settling velocity. This distance was chosen in accordance with measurements from other studies^{31–33}. For each polymer (PET, PVC and NP&A fibres), measurements were taken for clean and biofilmed particles under 3 salinities (SAL0, 18 and 30) and 3 sediment concentrations (100, 400 and 600 mg), resulting in 54 scenarios. Finally, to assess the impact of biofilm growth on settling velocity, measurements were taken at 0, 1, 2, 4 and 8 weeks for biofilmed PET fragments at SAL18 ($n = 216$). Images were analysed using a self-developed code in Matlab (R2020a)⁵⁷, see Supplementary Methods. Particle detection was made using the ‘imbinarize’ function available in Matlab, using global thresholding⁵⁸ or adaptive thresholding⁵⁹ depending on image characteristics. Particle properties, including area, were obtained using the ‘regionprops’ function. The velocities were obtained with self-developed cross-correlation-based particle tracking velocimetry (PTV) routines.

Statistical analysis. To understand the effects of microplastic condition (clean or biofilmed), salinity and clay concentration on settling velocity of microplastics, the combined interactions of [condition and salinity] and [condition and clay concentration] were assessed using generalised least square means analysis (two-sided). All statistical analysis was conducted using R Studio (R Core Team, 2013). Interactions were considered statistically significant if $p < 0.05$. Post hoc analysis was conducted using the lsmeans package, Tukey adjusted to understand significant differences between the least-squares means of specific variables by fitting linear models. For biofilm growth analysis from 0 to 8 weeks, a repeated-measures ANOVA (two-sided, comparison of means) was utilised after square root transformation to ensure equal variance (verified with Levene Test) and Tukey post hoc analysis. Before analysis, Shapiro–Wilk tests were applied to assess the normality.

Comparison to settling velocity predictions and formulae. As settling of microplastics has been related to the transitional flow regime, the formula of Ferguson and Church³⁷ for smooth, varied and angular grains was chosen for comparison of measured settling velocities:

$$w = \frac{RgD^2}{C_1v + (0.75C_2RgD^3)} \quad (1)$$

where w , mm s^{-1} denoted the particle’s settling velocity, R its submerged specific gravity, g , m s^{-2} the acceleration due to gravity, D , mm its diameter, v the kinematic viscosity, $\text{m}^2 \text{s}^{-1}$ of the fluid and where C_1 and C_2 are constants with changing empirical values depending on the type of particle as described by Ferguson and Church³⁷. For our comparisons shown in Fig. 4, the values angular grains were utilised where $C_1 = 24$ and $C_2 = 1.2$. Other C_1 and C_2 values were tested, but did not lower the overestimation of the calculated settling velocities. The measurements from the experiments and theoretical predictions were plotted in terms of settling velocity and equivalent diameter (D_e), mm:

$$D_e = 2\sqrt{\frac{A}{\pi}} \quad (2)$$

where mm^2 is area of the particle as the particle is assumed to be spherical. This is to determine whether settling predictions of microplastics using formula based on sediment dynamics is applicable for microplastic transport.

Reporting summary. Further information on research design is available in the Nature Portfolio Reporting Summary linked to this article.

Data availability

The data collected during this study can be accessed here: <https://doi.org/10.6084/m9.figshare.21473238.v1> and contains the results from the settling experiments for all scenarios and time trials (displacement, area, velocity) and the expected settling values calculated with Ferguson and Church.

Code availability

Please find the script to detect particles in images acquired with LabSFLOC camera and compute their size and settling velocity in the Supplementary Methods. The code was created in Matlab (R2020a).

Received: 4 April 2022; Accepted: 25 January 2023;

Published online: 11 February 2023

References

- Jambeck, J. R. et al. Plastic waste inputs from land into the ocean. *Science* **347**, 768–771 (2015).
- Eriksen, M. et al. Plastic pollution in the world’s oceans: more than 5 trillion plastic pieces weighing over 250,000 tons afloat at sea. *PLoS ONE* **9**, e111913 (2014).
- Lebreton, L. C. M. et al. River plastic emissions to the world’s oceans. *Nat. Commun.* **8**, 15611 (2017).
- Hoellein, T. J., Shogren, A. J., Tank, J. L., Risteca, P. & Kelly, J. J. Microplastic deposition velocity in streams follows patterns for naturally occurring allochthonous particles. *Sci. Rep.* **9**, 3740 (2019).
- Duan, J. et al. Weathering of microplastics and interaction with other coexisting constituents in terrestrial and aquatic environments. *Water Res.* **196**, 117011 (2021).
- Vroom, R. J. E., Koelmans, A. A., Besseling, E. & Halsband, C. Aging of microplastics promotes their ingestion by marine zooplankton. *Environ. Pollut.* **231**, 987–996 (2017).
- Hoellein, T., Rojas, M., Pink, A., Gasior, J. & Kelly, J. Anthropogenic litter in urban freshwater ecosystems: Distribution and microbial interactions. *PLoS ONE* **9**, e98485 (2014).
- Zhang, H. Transport of microplastics in coastal seas. *Estuarine Coastal Shelf Sci.* **199**, 74–86 (2017).
- Zettler, E. R., Mincer, T. J. & Amaral-Zettler, L. A. Life in the “plastisphere”: microbial communities on plastic marine debris. *Environ. Sci. Technol.* **47**, 7137–7146 (2013).
- Amaral-Zettler, L. A., Zettler, E. R. & Mincer, T. J. Ecology of the plastisphere. *Nat. Rev. Microbiol.* **18**, 139–151 (2020).
- Rummel, C. D., Jahnke, A., Gorokhova, E., Kühnel, D. & Schmitt-Jansen, M. Impacts of biofilm formation on the fate and potential effects of microplastic in the aquatic environment. *Environ. Sci. Technol. Lett.* **4**, 258–267 (2017).

12. Lagarde, F. et al. Microplastic interactions with freshwater microalgae: Hetero-aggregation and changes in plastic density appear strongly dependent on polymer type. *Environ. Pollut.* **215**, 331–339 (2016).
13. Chubarenko, I., Bagaev, A., Zobkov, M. & Esiukova, E. On some physical and dynamical properties of microplastic particles in marine environment. *Mar. Pollut. Bull.* **108**, 105–112 (2016).
14. Fazey, F. M. C. & Ryan, P. G. Biofouling on buoyant marine plastics: an experimental study into the effect of size on surface longevity. *Environ. Pollut.* **210**, 354–360 (2016).
15. Cooksey, K. E. & Wigglesworth-Cooksey, B. Adhesion of bacteria and diatoms to surfaces in the sea: a review. *Aquat. Microb. Ecol.* **9**, 87–96 (1995).
16. Manning, A. J., Baugh, J. V., Spearman, J. R. & Whitehouse, R. J. S. Flocculation settling characteristics of mud: sand mixtures. *Ocean Dyn.* **60**, 237–253 (2010).
17. Manning, A. J., Langston, W. J. & Jonas, P. J. C. A review of sediment dynamics in the Severn Estuary: influence of flocculation. *Mar. Pollut. Bull.* **61**, 37–51 (2010).
18. Cuthbertson, A. J. S., Samsami, F. & Dong, P. Model studies for flocculation of sand-clay mixtures. *Coast. Eng.* **132**, 13–32 (2018).
19. Long, M. et al. Interactions between microplastics and phytoplankton aggregates: Impact on their respective fates. *Mar. Chem.* **175**, 39–46 (2015).
20. Cunha, C., Faria, M., Nogueira, N., Ferreira, A. & Cordeiro, N. Marine vs freshwater microalgae exopolymers as biosolutions to microplastics pollution. *Environ. Pollut.* **249**, 372–380 (2019).
21. Besseling, E., Quik, J. T. K., Sun, M. & Koelmans, A. A. Fate of nano- and microplastic in freshwater systems: a modeling study. *Environ. Pollut.* **220**, 540–548 (2017).
22. Möhlenkamp, P., Purser, A. & Thomsen, L. Plastic microbeads from cosmetic products: an experimental study of their hydrodynamic behaviour, vertical transport and resuspension in phytoplankton and sediment aggregates. *Elem. Sci. Anth.* **6**, 61 (2018).
23. Andersen, T. J., Rominikan, S., Olsen, I. S., Skinnebach, K. H. & Fruergaard, M. Flocculation of PVC microplastic and fine-grained cohesive sediment at environmentally realistic concentrations. *Biol. Bull.* **240**, 42–51 (2021).
24. Mietta, F., Chassagne, C., Manning, A. J. & Winterwerp, J. C. Influence of shear rate, organic matter content, pH and salinity on mud flocculation. *Ocean Dyn.* **59**, 751–763 (2009).
25. Ivens Portela, L., Ramos, S. & Trigo Teixeira, A. Effect of salinity on the settling velocity of fine sediments of a harbour basin. *J. Coast. Res.* **165**, 1188–1193 (2013).
26. Manning, A. J. & Schoellhamer, D. H. Factors controlling floc settling velocity along a longitudinal estuarine transect. *Mar. Geol.* **345**, 266–280 (2013).
27. Li, Y. et al. Interactions between nano/micro plastics and suspended sediment in water: Implications on aggregation and settling. *Water Res.* **161**, 486–495 (2019).
28. Bagaev, A., Mizyuk, A., Khatmullina, L., Isachenko, I. & Chubarenko, I. Anthropogenic fibres in the Baltic Sea water column: field data, laboratory and numerical testing of their motion. *Sci. Total Environ.* **599–600**, 560–571 (2017).
29. Ballent, A., de Jesus Mendes, P., Pando, S., Thomsen, L. & Purser, A. Physical transport properties of marine microplastic pollution. *Biogeosci. Discuss* **9**, 18755–18798 (2012).
30. Kaiser, D., Kowalski, N. & Waniek, J. J. Effects of biofouling on the sinking behavior of microplastics. *Environ. Res. Lett.* **12**, 124003 (2017).
31. Khatmullina, L. & Isachenko, I. Settling velocity of microplastic particles of regular shapes. *Mar. Pollut. Bull.* **114**, 871–880 (2017).
32. Kowalski, N., Reichardt, A. M. & Waniek, J. J. Sinking rates of microplastics and potential implications of their alteration by physical, biological, and chemical factors. *Mar. Pollut. Bull.* **109**, 310–319 (2016).
33. Waldschläger, K. & Schüttrumpf, H. Effects of particle properties on the settling and rise velocities of microplastics in freshwater under laboratory conditions. *Environ. Sci. Technol.* **53**, 1958–1966 (2019).
34. Engelund, F. & Hansen, E. A monograph on sediment transport in alluvial streams. *Technical University of Denmark Ostervoldgade 10, Copenhagen K.* <https://repository.tudelft.nl/islandora/object/uuid:81101b08-04b5-4082-9121-861949c336c9> (1967).
35. Meyer-Peter, E. & Müller, R. Formulas for bed-load transport. In *IAHSR 2nd meeting, Stockholm, appendix 2. IAHR.* <https://repository.tudelft.nl/islandora/object/uuid:4fda9b61-be28-4703-ab06-43cdc2a21bd7?> (1948).
36. Van Rijn, L. & Kroon, A. Sediment transport by currents and waves. in *Proceedings of the Coastal Engineering Conference* 2613–2628 (American Society of Civil Engineers, 1993).
37. Ferguson, R. I. & Church, M. A simple universal equation for grain settling velocity. *J. Sediment. Res.* **74**, 933–937 (2004).
38. Van Melkebeke, M., Janssen, C. & De Meester, S. Characteristics and sinking behavior of typical microplastics including the potential effect of biofouling: implications for remediation. *Environ. Sci. Technol.* **54**, 8668–8680 (2020).
39. Ye, S. & Andradý, A. L. Fouling of floating plastic debris under Biscayne Bay exposure conditions. *Mar. Pollut. Bull.* **22**, 608–613 (1991).
40. Morét-Ferguson, S. et al. The size, mass, and composition of plastic debris in the western North Atlantic Ocean. *Mar. Pollut. Bull.* **60**, 1873–1878 (2010).
41. Rattanakawin, C. & Hogg, R. Aggregate size distributions in flocculation. *Colloids Surf. A Physicochem. Eng. Asp.* **177**, 87–98 (2001).
42. Wang, Z. et al. Settling velocity of irregularly shaped microplastics under steady and dynamic flow conditions. *Environ. Sci. Pollut. Res.* **28**, 62116–62132 (2021).
43. Mei, W. et al. Interactions between microplastics and organic compounds in aquatic environments: a mini review. *Sci. Total Environ.* **736**, 139472 (2020).
44. Corcoran, P. L. in *Handbook of Microplastics in the Environment* 531–542 (Springer, 2022).
45. Li, M., He, L., Zhang, X., Rong, H. & Tong, M. Different surface charged plastic particles have different cotransport behaviors with kaolinite particles in porous media. *Environ. Pollut.* **267**, 115534 (2020).
46. Harris, P. T. The fate of microplastic in marine sedimentary environments: a review and synthesis. *Mar. Pollut. Bull.* **158**, 111398 (2020).
47. Enders, K. et al. Tracing microplastics in aquatic environments based on sediment analogies. *Sci. Rep.* **9**, 15207 (2019).
48. Francalanci, S., Paris, E. & Solari, L. On the prediction of settling velocity for plastic particles of different shapes. *Environ. Pollut.* **290**, 118068 (2021).
49. Kane, I. A. & Clare, M. A. Dispersion, accumulation, and the ultimate fate of microplastics in deep-marine environments: a review and future directions. *Front. Earth Sci.* <https://doi.org/10.3389/feart.2019.00080> (2019).
50. Kooi, M., Van Nes, E. H., Scheffer, M. & Koelmans, A. A. Ups and downs in the ocean: effects of biofouling on vertical transport of microplastics. *Environ. Sci. Technol.* **51**, 7963–7971 (2017).
51. Schwarz, A. E., Lighthart, T. N., Boukris, E. & van Harmelen, T. Sources, transport, and accumulation of different types of plastic litter in aquatic environments: a review study. *Mar. Pollut. Bull.* **143**, 92–100 (2019).
52. Dris, R. et al. Microplastic contamination in an urban area: a case study in Greater Paris. *Environ. Chem.* **12**, 592–599 (2015).
53. Mekong River Commission. Measured total suspended solids@Can Tho. Mekong River Commission Data Portal. (2021).
54. Manning, A. J., Friend, P. L., Prowse, N. & Amos, C. L. Estuarine mud flocculation properties determined using an annular mini-flume and the LabSFLOC system. *Cont. Shelf Res.* **27**, 1080–1095 (2007).
55. Waldschläger, K., Lechthaler, S., Stauch, G. & Schüttrumpf, H. The way of microplastic through the environment – application of the source-pathway-receptor model (review). *Sci. Total Environ.* **713**, 136584 (2020).
56. Waldschläger, K., Born, M., Cowger, W., Gray, A. & Schüttrumpf, H. Settling and rising velocities of environmentally weathered micro- and macroplastic particles. *Environ. Res.* **191**, 110192 (2020).
57. MATLAB. MATLAB (MATLAB, 2020).
58. Otsu, N. A threshold selection method from gray-level histograms. *IEEE Trans. Syst. Man Cybern.* **SMC-9**, 62–66 (1979).
59. Bradley, D. & Roth, G. Adaptive thresholding using the integral image. *J. Graph. Tools* **12**, 13–21 (2007).

Author contributions

F.M.: conceptualisation, methodology, software (implementation), validation, formal analysis, investigation, writing—original draft, writing—review and editing, visualisation, project administration. R.F.: conceptualisation, methodology, software (designing and implementation), validation, formal analysis, resources, writing—review and editing, C.R.H.: conceptualisation, methodology, validation, writing—review and editing, supervision. C.W.: writing—review and editing, supervision. D.R.P.: conceptualisation, methodology, resources, writing—review and editing, supervision, funding acquisition.

Competing interests

The authors declare no competing interests.

Additional information

Supplementary information The online version contains supplementary material available at <https://doi.org/10.1038/s43247-023-00690-z>.

Correspondence and requests for materials should be addressed to Freija Mendrik.

Peer review information *Communications Earth & Environment* thanks Kryss Waldschläger and the other, anonymous, reviewer(s) for their contribution to the peer review of this work. Primary handling editors: Ilka Peeken and Clare Davis. Peer reviewer reports are available.

Reprints and permission information is available at <http://www.nature.com/reprints>

Publisher's note Springer Nature remains neutral with regard to jurisdictional claims in published maps and institutional affiliations.



Open Access This article is licensed under a Creative Commons Attribution 4.0 International License, which permits use, sharing, adaptation, distribution and reproduction in any medium or format, as long as you give appropriate credit to the original author(s) and the source, provide a link to the Creative Commons license, and indicate if changes were made. The images or other third party material in this article are included in the article's Creative Commons license, unless indicated otherwise in a credit line to the material. If material is not included in the article's Creative Commons license and your intended use is not permitted by statutory regulation or exceeds the permitted use, you will need to obtain permission directly from the copyright holder. To view a copy of this license, visit <http://creativecommons.org/licenses/by/4.0/>.

© The Author(s) 2023